Article

Halo-1,2,3-triazolium salts as halogen bond donors for the activation of imines in dihydropyridinone synthesis

Mikk Kaasik, Andrus Metsala, Sandra Kaabel, Kadri Kriis, Ivar Järving, and Tonis Kanger

J. Org. Chem., **Just Accepted Manuscript** • DOI: 10.1021/acs.joc.9b00248 • Publication Date (Web): 11 Mar 2019

Halo-1,2,3-triazolium salts as halogen bond donors for the activation of imines in dihydropyridinone synthesis

Mikk Kaasik, Andrus Metsala, Sandra Kaabel, Kadri Kriis, Ivar Järving and Tõnis Kanger*

Department of Chemistry and Biotechnology, Tallinn University of Technology, Tallinn 12618, Estonia

*E-mail: tonis.kanger@taltech.ee

Abstract: In the past decade halogen bond (XB) catalysis has gained considerable attention. Halo-triazoles are known XB donors, yet few examples detail their use as catalysts. As a continuation of our previous work the catalytic properties of substituted enantiomerically pure halo-triazolium salts were explored in the reaction between an imine and Danishefsky`s diene leading to the formation of dihydropyridinones. The catalytic activity of the XB donors was highly dependent on the choice of the halogen atom and on the counterion. Also, it was found that impurities in the diene affected the rate of the reaction.

Introduction

Halogen bonding is the process in which a Lewis acidic halogen atom interacts with a Lewis base.[1] It has been applied mainly in supramolecular chemistry and its use in solution is also growing.[2,3,4] Halogen bonds (XBs) are similar to hydrogen bonds (HBs), which have been extensively used in catalysis.[5] On the other hand, some properties of XBs can be considered more advantageous than HBs in catalysis, namely the high directionality of XBs and the use of soft donor atoms.[6,7] In 2008 Bolm *et al.* showed the potential of XBs in organocatalysis.[8] Since then there have been several reports describing the use of XBs to catalyse Diels-Alder,[9] Michael addition,[10] halogen abstraction[11] and other miscellaneous reactions.[12] In addition, computational studies have explored the catalytic potential of XB donors.[13] Nevertheless, the field is only starting to expand and even more importantly no examples of asymmetric catalysis based solely on XB activation have been reported. There are some examples of enantioselective reactions in which simultaneous different interactions, including XBs, are involved to achieve asymmetric induction.[14] Surprisingly, there are a limited number of examples utilizing halo-1,2,3-triazoles and their salts as catalysts, although these compounds are known XB donors,[9a,11b,11e,15] even more so, considering the ease of triazole synthesis via a copper-catalysed click reaction between alkyne and azide.[16] Easy access to a wide variety of chiral azides and the opportunities to modify the triazole ring make these compounds very attractive potential catalysts. The catalytic activity of the triazoles can be increased via quaternization, making the core of the triazole more electronegative and increasing the magnitude of the σ hole on the halogen atom.[15c,17] We have previously shown that chiral halogen substituted triazolium salts form complexes with imines and thioureas, and are additionally capable of enantiodiscrimination in solution.[18] To evaluate the catalytic potential of the triazolium salts, we used them in an aza-Diels-Alder[19] reaction between imine **1** and Danishefsky`s diene **2** (Scheme 1).

Scheme 1. The model reaction under study.

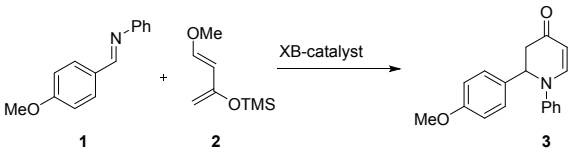

In this paper we demonstrate the high catalytic activity of the triazolium salts and describe how the catalytic activity is affected by the structure of the XB donor. In addition, an alternative mechanistic pathway for product formation is proposed and the importance of diene quality is described.

Results and Discussion

First, the set of synthesised XB donors was expanded compared to the one described in our previous publication[18] using the same general synthetic scheme (Figure 1).[20]

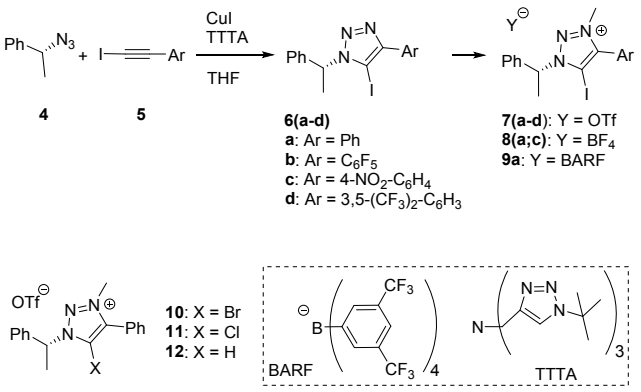

Figure 1.Triazolium salts used in the study.

The reaction of azide **4** derived from (*R*)-α-methyl benzyl amine and differently substituted aromatic 1-iodoalkynes **5** in the presence of copper(I)iodide and tris(1-*tert*-butyl-1*H*-1,2,3-triazolyl)methylamine (TTTA) afforded 5-iodo-1,2,3-triazole derivatives **6,** which were converted into triazolium salts **7** or tetrafluoroborate salts **8**. In addition, tetrakis-3,5-bis(trifluoromethyl)phenylborate (BARF) salt **9a** was also synthesised. Bromotriazole **10** was obtained starting from the corresponding bromoalkyne,[21] chloro derivative **11** via halogen exchange from **6a**[22] and hydrogen analogue **12** from the terminal alkyne (see Experimental Section for details). The substitution pattern of the phenyl ring involves various electronegative groups (**6b-d)**.

The electrostatic potential surfaces (ESP) of the triazoles and corresponding cationic structures (Table 1) were modelled to find

Table 1. The most positive electrostatic potential value VS,max (a.u.) (mapped on electron density isosurface of 0.001 a.u.) on the halogen atom X in the XB donor structure.[a]

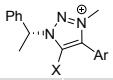

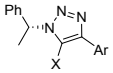

Entry	Ar	X	$V_{S,max}$	Entry	Ar	X	$V_{S,max}$
1	4-$NO_2C_6H_4$	I	0.1644	7	4-$NO_2C_6H_4$	I	0.0597
2	3,5-$(CF_3)_2C_6H_3$	I	0.1642	8	3,5-$(CF_3)_2C_6H_3$	I	0.0589
3	C_6F_5	I	0.1646	9	C_6F_5	I	0.0570
4	Ph	I	0.1565	10	Ph	I	0.0479
5	Ph	Br	0.1443	11	Ph	Br	0.0370
6	Ph	Cl	0.1350	12	Ph	Cl	0.0287

[a]The ESP values were modelled only for the cationic part of the XB donors **7a-d**, **10** and **11** to avoid the anion having an influence on the $V_{S,max}$ value on X and to evaluate the effect of the halogen atom, aromatic substituent and positive charge on the $V_{S,max}$ value.

structural factors that most influenced the σ hole. The DFT calculations were carried out with the Gaussian09 program[23] using the CAM-B3LYP[24] and M062X[25] functional with the DEF2TZVP[26] basis set. ESP values were calculated with the help of the Multiwfn program[27] and visualisation was made with the MOLEKEL[28] program. Charge has the most influence on the magnitude of the σ hole and similarly to previous results a positive charge of the triazole core increased the size of the σ hole on the halogen atom (Table 1, comparing entries 1-6 to entries 7-12).[15c,17] Next, the polarisability of the halogen atom had a smaller influence on the size of the σ hole (Table 1, comparing entries 4-6 or entries 10-12). The aromatic substituent of the triazole ring had a more subtle influence on the σ hole and can thus be used for the fine tuning of the properties of the catalyst (Table 1, entries 1-4).

Calculations show, in addition to the previously obtained affinity constant of $K_a(CDCl_3)$ = 8,[18] that halogen bonding between imine **1** and iodo-triazolium salt **7d** is plausible. Interestingly, in the minimum energy structure of **7d** the triflate counterion is not halogen bonded to the iodine atom (Figure 2, A). Based on

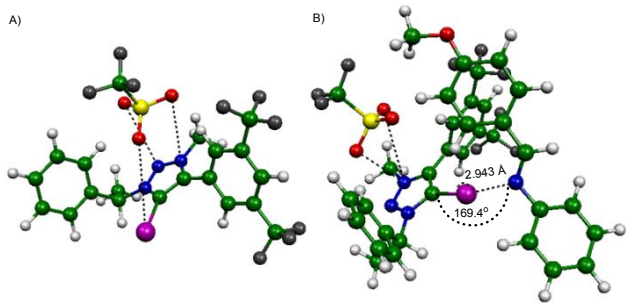

Figure 2. A) The most stable conformer of the XB donor 7d; B) the most stable conformer of 7d + 1 adduct.

solid state data we assumed that a XB to the counterion would be favoured.[18] This conformer is stable, but higher in energy (For further details, see SI Figure S2 and Table S1). When imine **1** is added to the **7d** system a stable adduct is formed containing an almost linear XB with an angle of 169.4° and a bond length of 2.943 Å (Figure 2, B). This data reveal that the activation of imine **1** by triazolium salt **7d** using a XB is plausible.

Based on previous results by Minakata *et al.*, the aza-Diels-Alder reaction between imine **1** and Danishefsky's diene **2** was chosen as a model reaction (Scheme 1).[9b] Since neutral triazoles **6** showed no catalytic activity in this reaction, they were omitted from the later part of the study. Proceeding to catalytic experiments, we also had to take into account the solubility of the donors in dichloromethane. Compounds **7d** and **8a** were not used as catalysts because of their poor solubility. Based on the previous, triflate **7a** was chosen as the reference catalyst in the study. A pentafluorophenyl group and a 4-nitrophenyl group have an influence on the σ hole comparable to that of a 3,5-bistrifluormethylphenyl group (Table 1, entries 1-3). Fortunately, the corresponding salts **7b** and **7c** were soluble in dichloromethane and could thus be used to probe the influence of the aromatic substituent on the reaction. Also, salts **8c**, **9a**, **10, 11** and **12** were included in the study to evaluate the influence of the counterion and halogen atom.

The reaction in the presence of triazolium salt **7a** gave promising results showing high conversion of imine **1** in a reasonable time. Although the triazolium salts were enantiomerically pure we observed no stereoselectivity in any of the following reactions. To get a better understanding of the reaction, we decided to run it in CD_2Cl_2 with 20 mol% of the catalyst and follow it by ^1H NMR, using *p*-xylene as an internal standard to determine the conversion. This change helped to reveal an unexpected lag period that preceded a rapid period of conversion of imine **1** to product **3** (Figure 3, purple line).

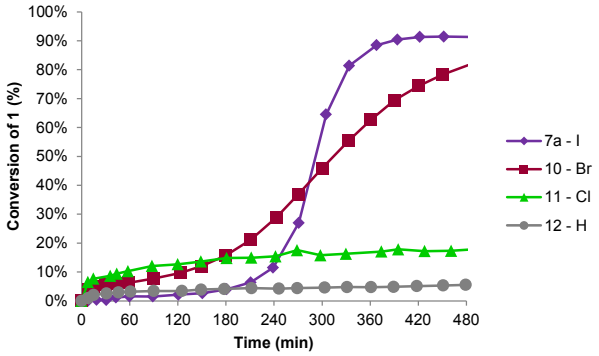

Figure 3. The dependence of the conversion of the model reaction on the halogen/hydrogen atom on the triazole ring of the catalyst.

Control experiments supported the idea that the reaction proceeded by XB activation. The hydrogen analogue **12** was markedly less active than **7a** (Figure 3, comparing purple and grey lines). After a few days only a moderate level of conversion was achieved. Also, no reaction took place if TBA-Cl was added to the reaction mixture with catalyst **7a**.[29] Bases have been successfully used to exclude the possibility of Brønsted acid catalysis.[9b,11f] Unfortunately, the product was not formed if K_2CO_3, Et_3N or Hünig's base was added to the reaction mixture. However, in all instances we observed the decomposition of **6a** into **12**. This indicates towards an unwanted interaction between the base and the XB catalyst. Therefore, the reactions in the presence of an added base were inconclusive and the possibility of hidden Brønsted acid catalysis could not be ruled out. Bromotriazole derivative **10** (Figure 3, magenta line) exhibited a similar reaction profile to **7a** with a gentler slope. The conversion of imine remained below 20% in the presence of chloro derivative **11** (Figure 3, green line) during the first eight hours. This is in agreement with our computations and previous results that have reported on the dependence of the XB donor ability on halogen atom polarisability.[11c,30] Elemental halogens might form in solution and act as the true catalysts. To rule this out, the reaction with bromotriazolium salt **10** was run in the presence of cyclohexene, which should quench free Br_2 and HBr.[10b,11d] Fortunately, we observed no change in reaction profile compared to the reaction with only **10** (For further details see SI Figure S4). In our opinion these results show that the catalytic activity comes from the halogen and the rest of the structure is relatively inactive.

The rate of the reaction was highly dependent on the quality and on the batch of the diene **2** used. The delay present in the reaction with **7a** was different in the case of various batches of diene (Figure 4, comparing the purple line to the others).

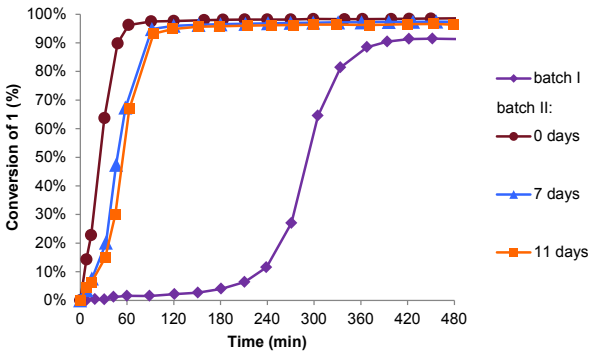

Figure 4. The influence of different batches of Danishefsky`s diene 2 and time after opening on the model reaction with catalyst 7a.

Also, the reaction was slower when the diene was used sometime after its first use (Figure 4, comparing the brown, orange and blue lines). Therefore all comparable studies were carried out with the same batch of diene in a minimal time frame. Although these findings significantly complicate the interpretation of data, we feel confident that general observations can still be made. The lag period, although shorter, was still present when different batches of diene were used with the catalyst **7a**. It was assumed that self-aggregation of the catalyst may also reduce its effective concentration in solution. We have observed the dependence of the chemical

shift values of the catalyst on its concentration (For further details, see SI Figure S5). Therefore the delay may have been caused by the kinetics of deaggregation to achieve sufficient concentration of the catalyst to activate imine **1**. Initially we assumed that product formation could increase the speed of deaggregation. To determine the influence of other reaction components on the catalyst, we incubated imine **1**, diene **2**, and product **3** in separate experiments with the catalyst for 30 minutes before adding the second reactant (For further details, see SI Figure S6).[31] Only in the case of incubation with the diene **2** was the reaction slower than the reference reaction and hence compounds **1** and **3** do not accelerate the reaction through facilitating deaggregation and exclude the possibility of autocatalysis.[32] On the other hand, diene **2** or its decomposition products might inhibit the catalyst. It is known that trimethylsilyl trifluoromethanesulfonate (TMSOTf) can catalyse Mannich[33] reaction and Diels-Alder reaction.[34] However, we did not detect the formation of TMSOTf by HRMS during the course of the reaction. Also, if TMSOTf is the actual catalyst then we should not observe any dependency of the reaction on the choice of halogen atom.

Next, the influence of the counterion on the catalytic activity was investigated (Figure 5). Surprisingly, compound **8c**

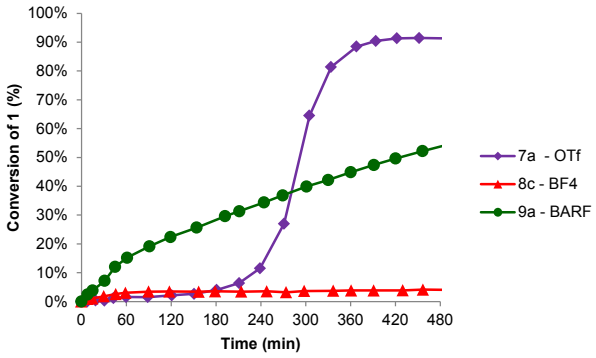

Figure 5. The dependence of the conversion of the model reaction on the counterion of the catalyst.

containing the tetrafluoroborate counterion was completely inactive (Figure 5, red line). The BARF counterion containing compound **9a** (Figure 5, green line) exhibited no delay at the start of the reaction. However, the reaction did not go to completion within eight hours. Both of these counterions are considered to be less coordinating than the triflate counterion and therefore compounds **8c** and **9a** should give a stronger XB with the imine.[35] Hence, these compounds should be more active than the triflate salt **7a**. Unusual and unpredictable influence of the counterion on the catalytic activity of the XB donors has also been described in earlier papers.[11c,36,37] The inactivity of **8c** can partly be explained by its lower stability in the reaction mixture compared to the others salts (For further details, see SI Figure S8). On the other hand, the absence of product formation again implies that the decomposition products were not catalytically active.

The influence of the aromatic substitution pattern of triflate salts **7a-c** on the reaction was investigated (Figure 6).

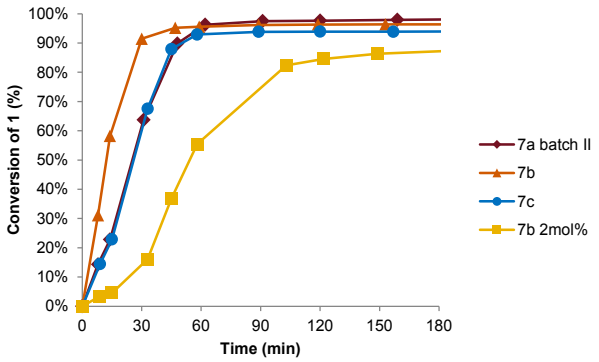

Figure 6. The influence of the aromatic substituent of the catalyst on the conversion of the model reaction.

Pentafluorophenyl derivative **7b** was a very efficient catalyst. The reaction was complete in almost 30 minutes (Figure 6, orange line). The lag period could not be observed but also not excluded on such a short time-scale with the better XB donor **7b** compared to donor **7a**. When we lowered the catalyst loading of **7b** from 20 to 2 mol% (Figure 6, yellow line), the lag period was again detected and the reaction profile was similar to that of the reaction with catalyst **7a**. The reaction was almost complete within 2 hours indicating high efficiency of the catalyst. *p*-nitrophenyl derivative **7c** was as active as catalyst **7a**.[38]

Finally, a more thorough study of NMR spectra revealed the formation of some new peaks that were converted into peaks corresponding to the product **3** during the course of the reaction (Figure 7). Based on HRMS and NMR analysis,

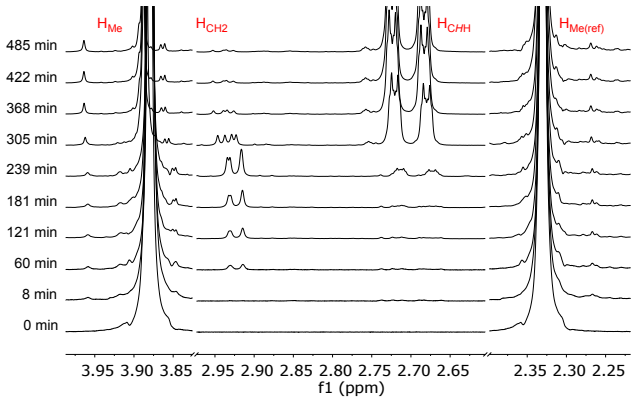

Figure 7. Outtake of 1H NMR spectra (CD_2Cl_2, 297 K, 400 MHz) from the reaction catalysed by 7a showing the methyl protons H_{Me} of 1, the methylene protons H_{CH2} of 14, one of the methylene protons H_{CHH} of 3, and the methyl protons $H_{Me(ref)}$ of *p*-xylene.

this compound could correspond to the Mannich intermediate **14** (Scheme 2, A).[39] It is assumed that the iodotriazolium salt **7** activates

Scheme 2. A) Mannich/Michael path to product 3; B) 4+2 cycloaddition path to product 3.

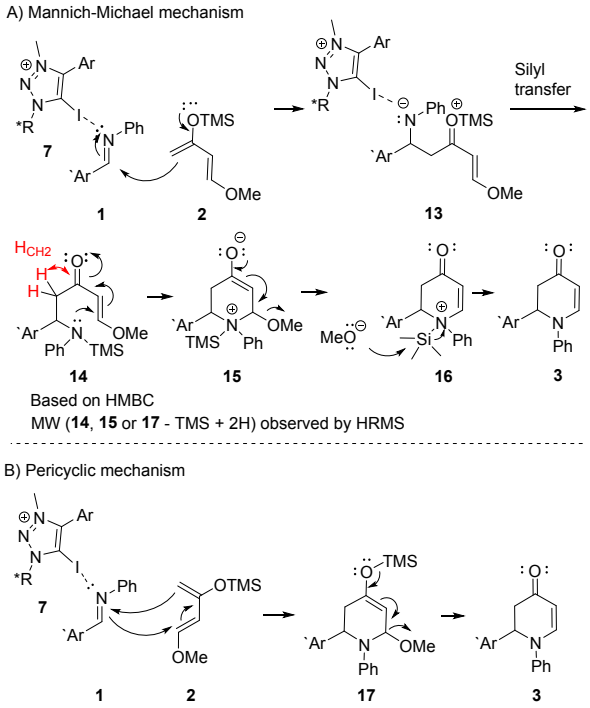

imine **1** towards a nucleophilic attack of silyl enol ether. Preliminary results by Minakata *et al.* also showed the feasibility of using a XB donor to catalyse the Mannich reaction.[9b] The intermediate **16** is formed by cyclization via an aza-Michael reaction followed by demethoxylation. The target compound **3** is obtained after desilylation. The initially expected 4+2 cycloaddition pathway could also be at work in parallel (Scheme 2, B).[40]

Conclusions

Halo-1,2,3-triazole-based XB donors were successfully used as catalysts to obtain dihydropyridinone **3**, although no enantioenriched products were formed. By modifying the structure of triazolium salts we were able to tune the catalytic properties of the XB donors to varying degrees. By introducing a pentafluorophenyl substituent, the catalyst loading could be lowered from 20 to 2 mol% without significant loss in activity. Both the choice of halogen atom and the counterion had a significant impact on the catalytic activity of the XB donors. Yet again, the counterion affected catalytic activity in an inexplicable way and therefore counterion effects in XB catalysis should receive closer examination. From a catalyst design perspective we are now interested in using different azides in the click reaction to move towards stereoselective XB catalysis. As the product might form through a tandem Mannich-Michael pathway, the catalytic potential of these compounds in the Mannich reaction could be of interest.

Experimental Section

All commercially available reagents were used without further purification. MeOH was dried by distillation over sodium metal. All air or moisture sensitive reactions were carried out under argon atmosphere using oven-dried glassware. The reactions were monitored by thin layer chromatography (TLC) with silica gel-coated aluminum plates (Merck 60 F254) and visualized with $KMnO_4$, anisaldehyde, vaniline or ninhydrine stain. Yields refer to chromatographically purified or crystallised products. ^{1}H NMR spectra were recorded on a Bruker Avance III instrument at 400 MHz and are reported in parts per million (δ) referenced to the residual solvent signal ($CDCl_3$ δ = 7.26, CD_3OD δ = 3.31 ppm, $[D_6]$DMSO δ = 2.50 ppm). Data for ^{1}H NMR spectra are as follows: chemical shift δ (ppm), multiplicity (s = singlet, bs = broad singlet, d = doublet, t = triplet, q = quartet, dd = doublet of doublets, m = multiplet), coupling constant J Hz, and relative integration. ^{13}C{^{1}H} NMR spectra were recorded at 101 MHz and are reported in parts per million (δ) referenced to the residual solvent signal ($CDCl_3$ δ = 77.16, CD_3OD δ = 49.00 ppm, $[D_6]$DMSO δ = 39.52 ppm). HRMS spectra were recorded with an Agilent Technologies 6540 UHD Accurate-Mass Q-TOF LC/MS spectrometer by using AJ-ESI ionization. Optical rotations were obtained with an Anton Paar GWB Polarimeter MCP500. IR spectra were recorded on a Bruker Tensor 27 FT-IR spectrophotometer. IR absorption frequencies in wavenumbers are listed, with the relative strength in parentheses (w = weak, m = medium, s = strong). (Iodoethynyl)benzene,[20] **4**,[41] **6a**,[18] **6d**,[18] **7a**[18] and **7d**[18] are known and were prepared following the literature procedure. A CEM Discover microwave reactor was used for the microwave assisted synthesis of (*R*)-5-chloro-4-phenyl-1-(1-phenylethyl)-1H-1,2,3-triazole. The reaction vessel was sealed with a Teflon cap and the reaction temperature was monitored by a non-contact infrared sensor.

(*R*)-5-iodo-4-(perfluorophenyl)-1-(1-phenylethyl)-1H-1,2,3-triazole (6b): 1-ethynyl-2,3,4,5,6-pentafluorobenzene: Bromopentafluoro-benzene (3.0 mL, 24.1 mmol), $PdCl_2(PPh_3)_2$ (0.342 g, 0.49 mmol), and CuI (0.187 g, 0.46 mmol) were dissolved in THF (60 mL). Hünig's base (16.0 mL, 89.9 mmol) was added, followed by ethynyltrimethylsilane (6.8 mL, 49.1 mmol), and the mixture was stirred for 24 h at 72 °C. The suspension was poured onto a pad of Celite®, washed with THF and the filtrate was concentrated under vacuum. Purification by flash column chromatography on silica gel (100% petroleum ether) afforded the Sonogashira coupling product and the Glaser coupling product as a mixture. The mixture was concentrated under vacuum and dissolved in MeOH (100 mL) and KOH (50%, 0.078 mL) was added. The reaction was stirred for 1 h, then quenched with H_2O (30 mL) and acidified with HCl (7 mL, 1M). The combined organic phase was dried over $MgSO_4$ and purification by distillation (130 °C, 1 atm) gave 1-ethynyl-2,3,4,5,6-pentafluorobenzene as an orange oil (0.74 g, 16% yield, solvent impurities were not completely removed). ^{1}H NMR (400 MHz, $CDCl_3$) δ 3.62 – 3.61 (m, 1H). 1,2,3,4,5-pentafluoro-6-(iodoethynyl)benzene: 1-ethynyl-2,3,4,5,6-pentafluorobenzene (0.30 g, 1.56 mmol), dissolved in THF (4 mL), was treated with CuI (0.029 g, 0.15 mmol) and 4-iodomorpholine hydroiodide (0.59 g, 2.0 mmol) and the reaction mixture was stirred for 3.5 h at rt. The suspension was poured onto a pad of neutral alumina, the solid phase was washed with THF and CH_2Cl_2, and the filtrate was concentrated under vacuum. The combined organic fractions were pooled and washed with a solution of $Na_2S_2O_3$ (100 mL, 5% w/w) and a solution of saturated NaCl (50 mL). The organic phase was dried over Na_2SO_4, concentrated and purified by column chromatography on silica gel (100% petroleum ether) to provide 1,2,3,4,5-pentafluoro-6-(iodoethynyl)benzene as an orange oil (0.35 g, 70% yield). ^{13}C{^{1}H} NMR (101 MHz, $CDCl_3$) δ 150.1 – 147.0 (m), 139.2 – 136.1 (m), 143.5 – 140.4 (m), 100.5 – 99.9 (m), 77.7 (q, J = 3.6 Hz), 21.7 (q, J = 3.9 Hz). **6b**: CuI (0.006 g, 0.032 mmol) and TTTA (0.015 mg, 0.035 mmol) were dissolved in freshly distilled THF (3.5 mL) under argon atmosphere and stirred at rt for 30 min. Then (*R*)-(1-azidoethyl)benzene (0.097 mL, 0.680 mmol) and 1,2,3,4,5-pentafluoro-6-(iodoethynyl)benzene (0.215 g, 0.676 mmol) were added and the reaction mixture was stirred at rt for 23 h. The reaction mixture was concentrated, NH_4OH (20 mL, 10% w/w) was added and the

aqueous phase was extracted with CH_2Cl_2 (2 x 25 mL). The combined organic phase was passed through a phase separator, concentrated and purified by column chromatography on silica gel (from 10% of EtOAc in petroleum ether) to provide triazole **6b** as colourless crystals (0.271 g, 86% yield). mp 157 – 160 °C; α_D^{20} 32.0 (*c* 0.21, $CHCl_3$); ^{1}H NMR (400 MHz, $CDCl_3$) δ 7.43 – 7.28 (m, 5H), 5.79 (q, *J* = 7.1 Hz, 1H), 2.14 (d, *J* = 7.1 Hz, 3H). ^{13}C{^{1}H} NMR (101 MHz, $CDCl_3$) δ 139.7, 129.2, 128.6, 126.7, 82.7, 62.3, 22.4. IR (KBr) v=: 1659 (w), 1554 (m), 1495 (s), 1413 (w), 1393 (w), 1238 (m), 1165 (m), 1126 (m), 1046 (m), 987 (s), 917 (w), 841 (s), 765 (m), 698 (s) cm^{-1}. HRMS (ESI/Q-TOF) m/z: [M + H]$^+$ Calcd for $C_{16}H_9F_5IN_3$ 465.9834**;** found: 465.9831.

(*R*)-5-iodo-4-(4-nitrophenyl)-1-(1-phenylethyl)-1H-1,2,3-triazole (6c): 1-(iodoethynyl)-4-nitrobenzene: Iodoform (4.10 g, 10.42 mmol), triphenylphosphine (2.87 g, 10.94 mmol) and *t*BuOK (1.11 g, 9.93 mmol) were added to THF (20 mL) under argon atmosphere. The suspension was stirred at rt for 5 minutes and turned brown. 4-nitrobenzaldehyde (0.75 g, 4.96 mmol) was added. After 30 minutes, the brown suspension was cooled to -78 °C and *t*BuOK (2.80 g, 24.95 mmol) was added. After an additional 30 minutes the reaction was quenched with brine (90 mL) at -78 °C. After warming to rt the two layers were separated and the aqueous phase was extracted with diethylether (3 x 90 mL). The combined organic phase was passed through a phase separator, concentrated and purified by column chromatography on silica gel (starting from 0% of EtOAc in petroleum ether) to provide the product as a yellow solid (1.17 g, 86% yield). ^{1}H NMR (400 MHz, $CDCl_3$) δ 8.24 – 8.15 (m, 2H), 7.62 – 7.54 (m, 2H). ^{13}C{^{1}H} NMR (101 MHz, $CDCl_3$) δ 147.5, 133.3, 130.1, 123.7, 92.5, 14.3. **6c:** CuI (0.006 g, 0.032 mmol) and TTTA (0.015 mg, 0.035 mmol) were dissolved in freshly distilled THF (3.5 mL) under argon atmosphere and stirred at rt for 30 min. Then 1-(iodoethynyl)-4-nitrobenzene (0.186 g, 0.681 mmol) and (*R*)-(1-azidoethyl)benzene (0.097 mL, 0.680 mmol) were added and the reaction mixture was stirred at rt for 5 h. The reaction mixture was concentrated, NH_4OH (20 mL, 10 % w/w) was added and the aqueous phase was extracted with CH_2Cl_2 (2 x 25 mL). The combined organic phase was dried over Na_2SO_4, filtered, concentrated and purified by column chromatography on silica gel (from 10% of EtOAc in petroleum ether) to provide triazole **6c** as yellow crystals (0.253 g, 88% yield). mp 153 °C dec in the presence of visible light; α_D^{20} 25.9 (*c* 0.16, $CHCl_3$); ^{1}H NMR (400 MHz, $CDCl_3$) δ 8.34 – 8.28 (m, 2H), 8.23 – 8.14 (m, 2H), 7.41 – 7.29 (m, 5H), 5.82 (q, *J* = 7.1 Hz, 1H), 2.14 (d, *J* = 7.1 Hz, 3H). ^{13}C{^{1}H} NMR (101 MHz, $CDCl_3$) δ 147.7, 147.6, 139.8, 136.8, 129.1, 128.6, 128.1, 126.7, 124.0, 78.3, 62.0, 22.5. IR (KBr) v=: 2992 (w), 2937 (w), 1602 (s), 1521 (s), 1458 (m), 1382 (m), 1346 (s), 1288 (m), 1245 (w), 1110 (m), 989 (m), 977 (m), 855 (s), 712 (s), 604 (w), 540 (w) cm^{-1}. HRMS (ESI/Q-TOF) m/z: [M + H]$^+$ Calcd for $C_{16}H_{13}IN_4O_2$ 421.0156**;** found: 421.0151.

(*R*)-5-bromo-4-phenyl-1-(1-phenylethyl)-1H-1,2,3-triazole: (bromoethynyl)benzene: To ethynylbenzene (0.75 mL, 6.85 mmol), dissolved in acetone (70 mL), were added NBS (1.35 g, 7.59 mmol) and $AgNO_3$ (0.119 g, 0.70 mmol). The resulting mixture was stirred at rt for 3.5 hours. The suspension was filtered and the filtrate was concentrated under reduced pressure. Then, the resulting crude mixture was added to water (50 mL) and extracted with Et_2O (3 × 50 mL). The combined organic phase was dried over K_2CO_3, concentrated and purified by column chromatography on silica gel (100% petroleum ether) to provide (bromoethynyl)benzene as a yellow oli (1.13 g, 91% yield). ^{1}H NMR (400 MHz, $CDCl_3$) δ 7.54 – 7.42 (m, 2H), 7.42 – 7.28 (m, 3H). ^{13}C{^{1}H} NMR (101 MHz, $CDCl_3$) δ 132.1, 128.8, 128.5, 122.8, 80.2, 49.9. The triazole: $Cu(OAc)_2$ (0.024 g, 0.132 mmol), CuBr (0.019 g, 0.132 mmol) and TTTA (0.058 mg, 0.135 mmol) were dissolved in freshly distilled THF (6.0 mL) under argon atmosphere and stirred at rt for 30 min. (bromoethynyl)benzene (0.239 g, 1.32 mmol) and (*R*)-(1-azidoethyl)benzene (0.194 g, 1.32 mmol) were added and the reaction mixture was stirred at 60 °C for two weeks. The reaction mixture was concentrated, NH_4OH (28 mL, 18 % w/w) was added and the aqueous phase was extracted with CH_2Cl_2 (3 x 30 mL). The combined organic phase was dried over anhydrous Na_2SO_4, concentrated

and purified by column chromatography on silica gel (from 10% of EtOAc in petroleum ether) to provide the Br-triazole as colourless crystals (0.176 g, 41% yield). α_D^{20} 27.0 (*c* 0.18, $CHCl_3$); ^1H NMR (400 MHz, $CDCl_3$) δ 8.00 – 7.95 (m, 2H), 7.48 – 7.41 (m, 2H), 7.41 – 7.28 (m, 6H), 5.78 (q, *J* = 7.1 Hz, 1H), 2.11 (d, *J* = 7.2 Hz, 3H). $^{13}C\{^1H\}$ NMR (101 MHz, $CDCl_3$) δ 144.8, 140.0, 129.8, 129.0, 128.7, 128.6, 128.4, 127.0, 126.6, 108.1, 60.0, 22.0. IR (KBr) v=: 3031 (w), 2988 (m), 2943 (w), 1607 (w), 1494 (m), 1477 (m), 1447 (m), 1374 (m), 1306 (w), 1280 (m), 1232 (s), 1049 (m), 989 (m), 975 (m), 771 (s), 733 (s), 698 (s), 536 (m) cm^{-1}. HRMS (ESI/Q-TOF) m/z: $[M + H]^+$ Calcd for $C_{16}H_{14}BrN_3$ 328.0444**;** found: 328.0439 (^{79}Br). The assignment is supported by an X-ray crystallographic structure.

(*R*)-5-chloro-4-phenyl-1-(1-phenylethyl)-1H-1,2,3-triazole: 6a (0.186 g, 0.496 mmol) was suspended in MeCN (1.5 mL) and EtOAc (0.5 mL) in a microwave vial, water (1.0 mL) and KCl (0.110 g, 1.47 mmol) were added to the mixture and the vial was sealed with a Teflon cap. The suspension of the reaction mixture was heated until most of the triazole **6a** was dissolved. The vial was placed into a microwave reactor and heated at 150 °C for 30 min. The reaction mixture was cooled, diluted with water and the aqueous phase was extracted with EtOAc (2 x 10 mL) and with DCM (3 x 10 mL). The combined organic phase was dried over anhydrous $MgSO_4$, concentrated and purified with column chromatography on silica gel (starting from 5% of EtOAc in petroleum ether) to provide the Cl-triazole as pale yellow crystals (0.115 g, 81% yield). mp 115 – 116 °C; α_D^{20} 22.6 (*c* 0.37, $CHCl_3$); ^1H NMR (400 MHz, $CDCl_3$) δ 8.00 – 7.94 (m, 2H), 7.49 – 7.41 (m, 2H), 7.40 – 7.28 (m, 6H), 5.75 (q, *J* = 7.1 Hz, 1H), 2.11 (d, *J* = 7.1 Hz, 3H). $^{13}C\{^1H\}$ NMR (101 MHz, $CDCl_3$) δ 142.1, 139.7, 129.5, 129.1, 128.8, 128.6, 128.5, 126.6, 126.5, 121.6, 59.1, 21.6. HRMS (ESI/Q-TOF) m/z: $[M + H]^+$ Calcd for $C_{16}H_{14}ClN_3$ 284.0949**;** found: 284.0954.

(*R*)-4-phenyl-1-(1-phenylethyl)-1H-1,2,3-triazole: CuI (0.010 g, 0.053 mmol) and TTTA (0.021 mg, 0.049 mmol) were dissolved in freshly distilled THF (3.5 mL) under argon atmosphere and stirred at rt for 30 min. Phenylacetylene (0.231 g, 1.013 mmol) and (*R*)-(1-azidoethyl)benzene (0.150 g, 1.019 mmol) dissolved in THF (2.0 mL) were added and the reaction mixture was stirred at rt for 21 h. The reaction mixture was concentrated, NH_4OH (20 mL, 10 % w/w) was added and the aqueous phase was extracted with CH_2Cl_2 (4 x 20 mL). The combined organic phase was dried over anhydrous Na_2SO_4, concentrated and purified by column chromatography on silica gel (starting from 0% of EtOAc in petroleum ether) to provide the H-triazole as colourless crystals (0.320 g, 84% yield). mp 115 – 116 °C; α_D^{20} -48.9 (*c* 0.20, $CHCl_3$); ^1H NMR (400 MHz, $CDCl_3$) δ 7.85 – 7.75 (m, 2H), 7.64 (s, 1H), 7.47 – 7.28 (m, 8H), 5.87 (q, *J* = 7.1 Hz, 1H), 2.03 (d, *J* = 7.1 Hz, 3H). $^{13}C\{^1H\}$ NMR (101 MHz, $CDCl_3$) δ 147.9, 140.0, 130.8, 129.2, 128.9, 128.7, 128.2, 126.7, 125.8, 118.5, 60.4, 21.5. IR (KBr) v=: 3121 (m), 3091 (w), 2985 (m), 1606 (w), 1496 (m), 1481 (m), 1463 (m), 1449 (m), 1356 (m), 1232 (m), 1219 (m), 1153 (m), 1075 (s),1026 (m), 992 (m), 916 (w), 818 (m), 764 (s), 714 (s), 692 (s), 521 (m) cm^{-1}. HRMS (ESI/Q-TOF) m/z: $[M + H]^+$ Calcd for $C_{16}H_{15}N_3$ 250.1339**;** found: 250.1336.

(*R*)-5-iodo-3-methyl-4-(perfluorophenyl)-1-(1-phenylethyl)-1H-1,2,3-triazol-3-ium trifluoromethanesulfonate (7b): Triazole **6b** (0.200 g, 0.230 mmol) was dissolved in CH_2Cl_2 (9.0 mL) under argon atmosphere. Methyl triflate (0.073 mL, 0.645 mmol) was added dropwise and the reaction mixture was stirred at rt for 21 h. After removal of the solvents under reduced pressure the solid was dissolved in CH_2Cl_2 (6.0 mL) and Et_2O (10.0 mL) was added to the solution and after 10 minutes a fine precipitate formed which was filtered to provide triflic salt **7b** as colourless crystals (0.231 g, 85% yield). mp 134 – 137 °C; α_D^{20} 12.6 (*c* 0.21, $CHCl_3$); ^1H NMR (400 MHz, $CDCl_3$) δ 7.49 – 7.37 (m, 5H), 6.10 (q, *J* = 6.9 Hz, 1H), 4.39 (s, 3H), 2.18 (d, *J* = 7.0 Hz, 3H). $^{13}C\{^1H\}$ NMR (101 MHz, $CDCl_3$) δ 136.2, 130.0, 129.8, 127.2, 120.6 (q, *J* = 320.4 Hz), 77.5, 67.5, 40.6, 21.7. IR (KBr) v=: 3034 (w), 1661 (m), 1505 (s), 1450 (m), 1246 (s), 1161 (s), 1078 (m), 1030 (s), 994 (s), 867 (m), 754 (m), 699 (m), 638 (s), 574 (w), 518 (m) cm^{-1}. HRMS (ESI/Q-TOF) m/z: $[M - CF_3O_3S]^+$ Calcd for $C_{17}H_{12}F_5IN_3$ 479.9991; found: 479.9998; $[OTf]^-$ Calcd for CF_3O_3S 148.9526; found 148.9550.

(*R*)-5-iodo-3-methyl-4-(4-nitrophenyl)-1-(1-phenylethyl)-1H-1,2,3-triazol-3-ium trifluoromethanesulfonate (7c): Triazole **6c** (0.102 g, 0.243 mmol) was dissolved in CH_2Cl_2 (5.0 mL) under argon atmosphere. Methyl triflate (0.041 mL, 0.363 mmol) was added dropwise and the reaction mixture was stirred at rt for 23 h. The reaction mixture was concentrated and dissolved in CH_2Cl_2 (1.5 mL). Et_2O (10.0 mL) was added to the reaction mixture and a precipitate formed after 20 minutes, which was filtered to provide triflic salt **7c** as colourless crystals (0.123 g, 87% yield). mp 84 – 87 °C; α_D^{20} 34.8 (*c* 0.25, MeOH); ^{1}H NMR (400 MHz, $CDCl_3$) δ 8.48 – 8.36 (m, 2H), 8.01 – 7.89 (m, 2H), 7.51 – 7.37 (m, 5H), 6.02 (q, *J* = 6.9 Hz, 1H), 4.32 (s, 3H), 2.19 (d, *J* = 7.0 Hz, 3H). ^{13}C{^{1}H} NMR (101 MHz, $CDCl_3$) δ 149.8, 145.4, 136.4, 132.1, 129.7, 129.6, 128.4, 127.1, 124.6, 120.5 (q, *J* = 320.0 Hz), 88.7, 67.0, 39.9, 21.6. IR (KBr) v=: 3107 (w), 1605 (m), 1527 (s), 1488 (w), 1454 (w), 1349 (s), 1277 (s), 1158 (s), 1030 (s), 856 (m), 757 (w), 704 (m), 638 (s), 600 (w), 574 (w) cm^{-1}. HRMS (ESI/Q-TOF) m/z: $[M - CF_3O_3S]^+$ Calcd for $C_{17}H_{16}IN_4O_2$ 435.0312; found 435.0327; $[OTf]^-$ Calcd for CF_3O_3S 148.9526; found 148.9549. The assignment is supported by an X-ray crystallographic structure.

(*R*)-5-iodo-3-methyl-4-phenyl-1-(1-phenylethyl)-1H-1,2,3-triazol-3-ium tetrafluoroborate (8a): Triazole **6a** (0.124 g, 0.330 mmol) was dissolved in CH_2Cl_2 (6.5 mL) under argon atmosphere. Trimethyloxonium tetrafluoroborate (0.061 mg, 0.412 mmol) was added and the reaction mixture was stirred at rt for 24 h. The reaction was quenched by adding MeOH (10.0 mL) and stirred for 1 h. After removal of the solvents under reduced pressure the crude produce was dissolved in MeOH (10.0 mL) and Et_2O (5.0 mL) was added to the solution and a fine precipitate formed which was filtered. The crystallisation was repeated a second time using MeOH (5.0 mL) and Et_2O (25.0 mL) to provide tetrafluoroboronic salt **8a** as colourless crystals (in total: 0.140 g, 89% yield). mp 193 – 195 °C; α_D^{20} 36.0 (*c* 0.16 in MeOH); ^{1}H NMR (400 MHz, CD_3OD) δ 7.77 – 7.57 (m, 5H), 7.55 – 7.37 (m, 5H), 6.23 (q, *J* = 6.9 Hz, 1H), 4.27 (s, 3H), 2.12 (d, *J* = 6.9 Hz, 3H). ^{13}C{^{1}H} NMR (101 MHz, CD_3OD) δ 148.6, 138.8, 133.1, 131.4, 130.7, 130.4, 130.3, 128.2, 124.3, 91.3, 67.4, 39.8, 22.0. HRMS (ESI/Q-TOF) m/z: $[M - BF_4]^+$ Calcd for $C_{17}H_{17}IN_3$ 390.0462; found 390.0455; $[BF_4]^-$ Calcd for BF_4: 86.0071; found 86.0072 (^{10}B), 87.0037 (^{11}B). The assignment is supported by an X-ray crystallographic structure.

(*R*)-5-iodo-3-methyl-4-(4-nitrophenyl)-1-(1-phenylethyl)-1H-1,2,3-triazol-3-ium tetrafluoroborate (8c): Triazole **6c** (0.112 g, 0.267 mmol) was dissolved in CH_2Cl_2 (5.5 mL) under argon atmosphere. Trimethyloxonium tetrafluoroborate (0.055 mg, 0.372 mmol) was added and the reaction mixture was stirred at rt for 3 days. The reaction was quenched by adding MeOH (5.5 mL) and stirred for 40 min. After removal of the solvents under reduced pressure the solid was dissolved in CH_2Cl_2 (2.0 mL) and Et_2O (5.0 mL) was added to the solution and a precipitate formed after 20 minutes, which was filtered to provide tetrafluoroboronic salt **8c** as pale yellow crystals (0.132 g, 95% yield). mp 98 – 101 °C; α_D^{20} 39.4 (*c* 0.19, MeOH); ^{1}H NMR (400 MHz, CD_3OD) 8.56 – 8.45 (m, 2H), 8.01 – 7.88 (m, 2H), 7.56 – 7.36 (m, 5H), 6.25 (q, *J* = 6.9 Hz, 1H), 4.32 (s, 3H), 2.13 (d, *J* = 6.9 Hz, 3H). ^{13}C{^{1}H} NMR (101 MHz, CD_3OD) δ 151.3, 146.9, 138.7, 133.2, 130.38, 130.37, 130.3, 128.2, 125.5, 92.1, 67.6, 40.0, 22.0. IR (KBr) v=: 1605 (w), 1526 (s), 1487 (w), 1453 (w), 1348 (s), 1287 (w), 1061 (s), 855 (m), 763 (w), 704 (m), 600 (w) cm^{-1}. HRMS (ESI/Q-TOF) m/z: $[M - BF_4]^+$ Calcd for $C_{17}H_{16}IN_4O_2$ 435.0312; found 435.0315; $[BF_4]^-$ Calcd for BF_4 86.0071; found: 86.0089 (^{10}B), 87.0054 (^{11}B). The assignment is supported by an X-ray crystallographic structure.

(*R*)-5-iodo-3-methyl-4-phenyl-1-(1-phenylethyl)-1H-1,2,3-triazol-3-ium tetrakis3,5-bis(trifluoromethyl)phenylborate (9a): Sodium tetrakis3,5-bis(trifluoromethyl)phenylborate: A three-neck round bottom flask fitted with a reflux condenser was evacuated, flame dried and filled with argon prior to use. Magnesium (1.11 g, 45.7 mmol), $NaBF_4$ (0.71 g, 6.4 mmol) and Et_2O (150 mL) were added to the flask. To start the reaction dibromoethane (0.49 mL, 5.7 mmol) was added and the flask was heated for 5 minutes followed by the dropwise addition of 3,5-bis(trifluoromethyl)bromobenzene (5.0 mL, 35.9 mmol) dissolved in Et_2O (40 mL)

over 70 min. The solution was then stirred over night at rt. As all of the magnesium had not reacted the reaction was refluxed for an additional 24 h. Then the reaction mixture was quenched by the addition of Na_2CO_3 (16.2 g, 153 mmol) dissolved in H_2O (200 mL) and stirred for 1 h and filtered. The aqueous phase was extracted three times with Et_2O (50 mL), the combined organic phase was dried over Na_2SO_4. The solvent was removed and the remaining crude product was dissolved in toluene (50 mL) and concentrated to remove remaining traces of water, this was repeated three more times. The product was dried under reduced pressure with heating (100 °C) for 10 h to yield a brown solid. This solid was washed with CH_2Cl_2 and toluene, dried under reduced pressure with heating (100 °C) in the presence of P_2O_5 for 2 days to yield the NaBARF as a pale grey solid (2.70 g, 47% yield). ^{1}H NMR (400 MHz, [D$_6$]DMSO) δ 7.64 (s, 4H), 7.61 (s, 8H). ^{13}C{^{1}H} NMR (101 MHz, [D$_6$]DMSO) δ 161.0 (q, J = 49.9 Hz), 134.9, 129.1 – 127.9 (m), 124.0 (q, J = 272.2 Hz), 118.0 – 117.1 (m). Tetramethylammonium tetrakis3,5-bis(trifluoromethyl)-phenylborate: NaBARF (1.76 g, 1.99 mmol) was suspended in CH_2Cl_2 (100 mL) and tetramethylammonium iodide (0.60 g, 2.98 mmol) was added and the reaction mixture was stirred at rt for 3 days open to air (moisture helps to increase the solubility of NaBARF). Then the mixture was filtered and the filtrate concentrated under reduced pressure. The obtained solid was suspended in Et_2O and then filtered (to remove excess Me_4NI). The filtrate was concentrated under reduced pressure and the resulting solid was recrystallised from CH_2Cl_2 at 0 °C for three times to yield the tetramethylammonium BARF salt as a colourless powder (in total: 1.49 g, 80% yield). ^{1}H NMR (400 MHz, [D$_6$]DMSO) δ 7.66 (s, 4H), 7.64 – 7.57 (m, 8H), 3.10 (s, 12H). ^{13}C{^{1}H} NMR (101 MHz, [D$_6$]DMSO) δ 161.0 (q, J = 49.9 Hz), 134.0 (s), 129.1 – 127.9 (m), 124.0 (q, J = 272.4 Hz). 117.9 – 117.27 (m), 54.7 – 54.0 (m). **9a:** Triazolium **7a** (0.153 g, 0.284 mmol) was dissolved in a mixture of CH_2Cl_2 (17.4 mL) and MeOH (5.8 mL), tetramethylammonium BARF (0.293 g, 0.313 mmol) was added and the reaction mixture was stirred at rt for 22 h. After removal of the solvents under reduced pressure the precipitate was suspended in Et_2O (11.5 mL) and stirred for 45 minutes at 0 °C. The precipitate was removed by filtration and the filtrate was concentrated. The obtained solid was suspended in $CHCl_3$ (11.5 mL) and stirred for 30 minutes at 0 °C. The precipitate was removed by filtration and the filtrate was concentrated under reduced pressure to provide BARF salt **9a** as colourless crystals (0.342 g, 96% yield). mp 173 – 174 °C; α_D^{20} 12.5 (c 0.37, $CHCl_3$); ^{1}H NMR (400 MHz, $CDCl_3$) δ 7.67 – 7.56 (m, 9H), 7.53 – 7.47 (m, 2H), 7.43 (s, 4H), 7.39 – 7.30 (m, 3H), 7.30 – 7.25 (m, 2H), 7.24 – 7.19 (m, 2H), 5.87 (q, J = 7.0 Hz, 1H), 4.04 (s, 3H), 1.99 (d, J = 7.0 Hz, 3H). ^{13}C{^{1}H} NMR (101 MHz, $CDCl_3$) δ 161.8 (q, J = 49.9 Hz), 147.9, 135.1 – 134.8 (m), 135.0, 133.5, 130.7, 130.5, 130.0, 129.7 – 128.5 (m), 129.3, 127.0, 124.63 (q, J = 272.6 Hz), 120.6, 117.8 – 117.5 (m), 86.4, 67.7, 39.5, 21.3. IR (KBr) v=: 1610 (m), 1355 (s), 1277 (s), 1131 (s), 888 (m), 839 (m), 763 (w), 745 (m), 715 (m), 697 (m), 683 (m), 670 (m) cm^{-1}. HRMS (ESI/Q-TOF) m/z: [M – $C_{32}H_{12}BF_{24}$]$^+$ Calcd for $C_{17}H_{17}IN_3$ 390.0462; found 390.0460; [BARF]$^-$: Calcd for $C_{32}H_{12}BF_{24}$ 862.0691; found 862.0696 (^{10}B).

(*R*)-5-bromo-3-methyl-4-phenyl-1-(1-phenylethyl)-1H-1,2,3-triazol-3-ium trifluoromethanesulfonate (10): The Br-triazole (0.096 g, 0.29 mmol) was dissolved in CH_2Cl_2 (6.0 mL) under argon atmosphere. Methyl triflate (0.050 mL, 0.439 mmol) was added dropwise and the reaction mixture was stirred at rt for 22 h. After removal of the solvents under reduced pressure the product was purified by column chromatography on silica gel (from 5% of MeOH in CH_2Cl_2) to provide triflic salt **10** as an off colourless oil (0.049 g, 34% yield). α_D^{20} -1.6 (c 0.18, $CHCl_3$); ^{1}H NMR (400 MHz, $CDCl_3$) δ 7.70 – 7.55 (m, 5H), 7.49 – 7.37 (m, 5H), 6.06 (q, J = 7.0 Hz, 1H), 4.31 (s, 3H), 2.19 (d, J = 7.0 Hz, 3H). ^{13}C{^{1}H} NMR (101 MHz, $CDCl_3$) δ 143.2, 136.6, 132.4, 130.2, 129.8, 129.8, 129.7, 127.1, 122.4, 120.8 (q, J = 320.4 Hz), 116.5, 65.4, 39.9, 21.3. IR (film) v=: 3063 (w), 1566 (w), 1493 (m), 1455 (m), 1266 (s), 1225 (m),

1154 (s), 1031 (s), 795 (w), 760 (m), 702 (s), 638 (s), 573 (w) cm^{-1}. HRMS (ESI/Q-TOF) m/z: $[M - CF_3O_3S]^+$ Calcd for $C_{17}H_{17}BrN_3$ 342.0600; found 342.0601 (^{79}Br); $[OTf]^-$ Calcd for CF_3O_3S 148.9526; found 148.9525.

(*R*)-5-chloro-3-methyl-4-phenyl-1-(1-phenylethyl)-1H-1,2,3-triazol-3-ium trifluoromethanesulfonate (11): Triazole **11** (0.1005 g, 0.354 mmol) was dissolved in CH_2Cl_2 (6.0 mL) under argon atmosphere. Methyl triflate (0.060 mL, 0.531 mmol) was added dropwise and the reaction mixture was stirred at rt for 23 h. After removal of the solvents under reduced pressure the product was mixed overnight in MeOH (1 mL) in the presence of activated charcoal (0.025 g) to remove some of the coloured impurities. In addition **11** was purified by column chromatography on silica gel (from 5% of MeOH in CH_2Cl_2) to provide triflic salt **11** as a colourless oil (0.132 g, 83% yield. α_D^{20} -15.5 (*c* 0.27, $CHCl_3$); ^1H NMR (400 MHz, $CDCl_3$) δ 7.63 – 7.49 (m, 5H), 7.43 – 7.28 (m, 5H), 6.00 (q, *J* = 7.0 Hz, 1H), 4.24 (s, 3H), 2.14 (d, *J* = 7.0 Hz, 3H). $^{13}C\{^1H\}$ NMR (101 MHz, $CDCl_3$) δ 140.5, 136.4, 132.5, 130.1, 129.9, 129.8, 129.7, 129.2, 127.0, 120.7, 64.4, 40.0, 20.9. IR (film) v=: 1494 (w), 1455 (w), 1266 (s), 1225 (m), 1155 (s), 1032 (s), 761 (m), 701 (m), 638 (s), 574 (w) cm^{-1}. HRMS (ESI/Q-TOF) m/z: $[M - CF_3O_3S]^+$ Calcd for $C_{17}H_{17}ClN_3$ 298.1106; found 298.1110; $[OTf]^-$ Calcd for CF_3O_3S 148.9526; found 148.9544.

(*R*)- 3-methyl-4-phenyl-1-(1-phenylethyl)-1H-1,2,3-triazol-3-ium trifluoromethanesulfonate (12): (*R*)-4-phenyl-1-(1-phenylethyl)-1*H*-1,2,3-triazole (0.050 g, 0.201 mmol) was dissolved in CH_2Cl_2 (4.0 mL) under argon atmosphere. Methyl triflate (0.045 mL, 0.401 mmol) was added dropwise and the reaction mixture was stirred at rt for 21 h After removal of the solvents under reduced pressure the product was purified by column chromatography on silica gel (from 3% of MeOH in CH_2Cl_2) to provide triflic salt **12** as a colourless oil (0.074 g, 89% yield). α_D^{20} -27.6 (*c* 0.09, $CHCl_3$); ^1H NMR (400 MHz, $CDCl_3$) δ 8.54 (s, 1H), 7.63 – 7.50 (m, 7H), 7.48 – 7.38 (m, 3H), 6.17 (q, *J* = 7.1 Hz, 1H), 4.26 (s, 3H), 2.11 (d, *J* = 7.0 Hz, 3H). $^{13}C\{^1H\}$ NMR (101 MHz, $CDCl_3$) δ 143.6, 136.7, 132.1, 130.0, 129.8, 129.7, 129.6, 128.0, 127.7, 122.0, 120.9 (q, *J* = 320.3 Hz), 65.4, 38.8, 20.3. HRMS (ESI/Q-TOF) m/z: $[M - CF_3O_3S]^+$ Calcd for $C_{17}H_{18}N_3$ 264.1495; found 264.1502; $[OTf]^-$ Calcd for CF_3O_3S: 148.9526; found 148.9551.

General procedure for the reactions with ^1H NMR monitoring between **1** and **2**: All of the crystallised XB donors were additionally purified by column chromatography (from 5% of MeOH in CH_2Cl_2) before their use in the catalytic experiments. Danishefsky`s diene of purity 96% was purchased from Alfa Aesar and used as received. (*E*)-1-(4-methoxyphenyl)-*N*-phenylmethanimine **1**: $MgSO_4$ (6.8 g, 56.4 mmol) was suspended in CH_2Cl_2 (13 mL), then *p*-anysaldehyde (1.8 mL, 13.8 mmol) and aniline (1.2 mL, 13.1 mmol) were added. The reaction mixture was stirred at rt for 24 h and filtered. After removal of the solvent under reduced pressure, the crude product was purified by crystallisation from a mixture of CH_2Cl_2 and Et_2O to yield imine **1** as colourless crystals (1.94 g, 70% yield). ^1H NMR (400 MHz, $CDCl_3$) δ 8.40 (s, 1H), 7.93 – 7.79 (m, 2H), 7.40 (dd, *J* = 8.7, 6.9 Hz, 2H), 7.22 (td, *J* = 7.6, 7.2, 1.5 Hz, 3H), 7.04 – 6.93 (m, 2H), 3.87 (s, 3H). $^{13}C\{^1H\}$ NMR (101 MHz, $CDCl_3$) δ 162.3, 159.8, 152.5, 130.6, 129.4, 129.2, 125.7, 121.0, 114.3, 55.5.

The XB donor (0.052 mmol, 0.2 equiv.) was dissolved in a stock solution of CD_2Cl_2 (0.650 mL) containing imine **1** (0.4 M, 1.0 equiv.) and *p*-xylene (0.2 M, 0.5 equiv.). Then 0.600 mL of the solution was transferred to a NMR tube and the ^1H spectrum was measured. Then Danishefsky`s diene **2** (0.063 mL, 1.3 equiv.) was added and the ^1H spectra were measured at approximately 8, 15 and 30 minute intervals for at least the first 8 h of the reaction. In certain cases the product **3** was isolated by purification with column chromatography on silica gel (from 20% of EtOAc in petroleum ether) to provide **3** as a yellow oil with yields usually 10% lower than the corresponding conversion.

Parameters specific to the experiment: T = 297 K, Relaxation delay = 36 s, Number of Scans = 8. Data Processing was performed using MestreNova. The spectra were phased, baseline-corrected and zero-filled (To spectrum size 128K). Then line fitting function (deconvolution) was used to more accurately integrate the peaks corresponding to the protons of the methoxy group of imine **1** and methyl group of *p*-xylene.

2-(4-methoxyphenyl)-1-phenyl-2,3-dihydropyridin-4(1H)-one (3): ^{1}H NMR (400 MHz, $CDCl_3$) δ 7.64 (dd, J = 7.8, 1.2 Hz, 1H), 7.35 – 7.27 (m, 2H), 7.21 – 7.15 (m, 2H), 7.15 – 7.07 (m, 1H), 7.07 – 7.00 (m, 2H), 6.90 – 6.81 (m, 2H), 5.32 – 5.26 (m, 1H), 5.24 (dd, J = 6.9, 3.2 Hz, 1H), 3.76 (s, 3H), 3.26 (dd, J = 16.3, 7.0 Hz, 1H), 2.75 (ddd, J = 16.3, 3.3, 1.2 Hz, 1H). ^{13}C{^{1}H} NMR (101 MHz, $CDCl_3$) δ 190.5, 159.2, 148.3, 144.8, 129.9, 129.6, 127.5, 124.5, 118.8, 114.4, 102.9, 61.4, 55.4, 43.7.

Acknowledgements

The authors thank the Estonian Ministry of Education and Research (Grant Nos. IUT 19-32, IUT 19-9, PUT692 and PUT1468) and the Centre of Excellence in Molecular Cell Engineering 2014-2020.4.01.15-0013 for financial support. This work has been partially supported by ASTRA “TUT Institutional Development Programme for 2016-2022” Graduate School of Functional Materials and Technologies" (2014-2020.4.01.16-0032). We thank Dr. Marina Kudrjašova for the ^{19}F NMR measurmetns, Dr. Riina Aav for advice on the NMR experiments, Dr. Aleksander-Mati Müürisepp for IR and Ms. Jevgenija Martõnova for the X-ray measurements.

Supporting Information

Copies of ^{1}H and ^{13}C{^{1}H} spectra, spectra and chromatograms used for the mechanistic study, computational details and crystallographic details.

REFERENCES

[1] Desiraju, G. R.; Ho, P. S.; Kloo, L.; Legon, A. C.; Marquardt, R.; Metrangolo, P.; Politzer, P.; Resnati, G.; Rissanen, K. Definition of the halogen bond (IUPAC Recommendations 2013). *Pure Appl. Chem*. **2013,** *85*, 1711–1713.

[2] For general reviews see: b) Montaña, Á. M. The σ and π Holes. The Halogen and Tetrel Bondings: Their Nature, Importance and Chemical, Biological and Medicinal Implications. *ChemistrySelect* **2017,** *2*, 9094–9112; b) Cavallo, G.; Metrangolo, P.; Milani, R.; Pilati, T.; Priimagi, A.; Resnati, G.; Terraneo, G. The Halogen Bond. *Chem. Rev.* **2016,** *116*, 2478–2601; c) Wang, H.; Wang, W.; Jin, W. J. σ-Hole Bond vs π-Hole Bond: A Comparison Based on Halogen Bond. *Chem. Rev*. **2016**, *116*, 5072–5104; d) Gilday, L. C.; Robinson, S. W.; Barendt, T. A.; Langton, M. J.; Mullaney, B. R.; Beer, P. D. Halogen Bonding in Supramolecular Chemistry. *Chem. Rev*. **2015**, *115*, 7118–7195.

[3] For reviews focusing on the use of XBs in crystal engineering: a) Christopherson, J.-C.; Topić, F.; Barrett, C. J.; Friščič, T. Halogen-Bonded Cocrystals as Optical Materials: Next-Generation Control over Light–Matter Interactions. *Cryst. Growth Des.* **2018**, *18*, 1245−1259; b) Li, B.; Zang, S.-Q.; Wang, L.-Y.; Mak, T. C. W. Halogen bonding: A powerful, emerging tool for constructing high-dimensional metal-containing supramolecular networks. *Coord. Chem. Rev*. **2016**, *308,* 1–21; c) Berger, G.; Soubhyea, J.; Meyer, F. Halogen bonding in polymer science: from crystal engineering to functional supramolecular polymers and materials. *Polym. Chem*. **2015**, *6*, 3559–3580; d) Mukherjee, A.; Tothadi, S.; Desiraju, G. R. Halogen Bonds in Crystal Engineering: Like Hydrogen Bonds yet Different. *Acc. Chem. Res*. **2014**, *47*, 2514–2524.

[4] For reviews focusing on the use of XBs in solution: a) Tepper, R.; Schubert, U. S. Halogen Bonding in Solution: Anion Recognition, Templated Self-Assembly, and Organocatalysis. *Angew. Chem. Int. Ed.* **2018**, 57, 6004–6016; b) Brown, A.; Beer, P. D. Halogen bonding anion recognition. *Chem. Commun*. **2016**, *52*, 8645–8658; c) Jentzsch, A. V. Applications of halogen bonding in solution. *Pure Appl. Chem*. **2015**, *87*,15–41; d) Carlsson, A.-C.C.; Vega, A.X.; Erdélyi, M. Halogen Bonding in Solution. *Top. Curr.Chem.* **2015**, *359*, 49–76; e) Beale, T. M.; Chudzinski, M. G.; Sarwar, M. G.; Taylor, M. S. Halogen bonding in solution: thermodynamics and applications. *Chem. Soc. Rev*. **2013**, *42*, 1667–1680.

[5] For reviews, see: a) Nishikawa, Y. Recent topics in dual hydrogen bonding catalysis. *Tetrahedron Lett.* **2018**, *59*, 216-223; b) Zhao, B.-L.; Li, J.-H.; Du, D.-M. Squaramide-Catalyzed Asymmetric Reactions. *Chem. Rec*. **2017**, *17*, 994–1018; c) Fang, X.; Wang, C.-J.

Recent advances in asymmetric organocatalysis mediated by bifunctional amine–thioureas bearing multiple hydrogen-bonding donors. *Chem. Commun*. **2015**, *51*, 1185–1197; d) Chauhan, P.; Mahajan, S.; Kaya, U.; Hack, D.; Enders, D. Bifunctional Amine-Squaramides: Powerful Hydrogen-Bonding Organocatalysts for Asymmetric Domino/Cascade Reactions. *Adv. Synth. Catal*. **2015**, *357*, 253–281; e) Albrecht, Ł.; Jiang, H.; Jørgensen, K. A. Hydrogen-Bonding in Aminocatalysis: From Proline and Beyond. *Chem. Eur. J*. **2014**, *20*, 358–368.

[6] a) Rissanen, K. Halogen bonded supramolecular complexes and networks. *CrystEngComm* **2008**, *10*, 1107–1113; b) Lommerse, J. P. M.; Stone, A. J.; Taylor, R.; Allen, F. H. The Nature and Geometry of Intermolecular Interactions between Halogens and Oxygen or Nitrogen. *J. Am. Chem. Soc*. **1996**, *118*, 3108–3116.

[7] a) Riel, A. M. S.; Jessop, M. J.; Decato, D. A.; Massena, C. J.; Nascimento, V. R.; Berryman, O. B. Experimental investigation of halogen-bond hard–soft acid–base complementarity. *Acta Crystallogr., Sect. B: Struct. Sci., Cryst. Eng. Mater.* **2017**, *73*, 203–209; b) Robertson, C. C.; Perutz, R. N.; Brammer, L.; Hunter, C. A. A solvent-resistant halogen bond. *Chem. Sci*. **2014**, *5*, 4179–4183.

[8] Bruckmann, H. A.; Pena, M. A.; Bolm, C. Organocatalysis through Halogen-Bond Activation. *Synlett* **2008**, 900–902.

[9] a) Haraguchi, R.; Hoshino, S.; Sakai, M.; Tanazawa, S.; Morita, Y.; Komatsu, T.; Fukuzawa, S. Bulky iodotriazolium tetrafluoroborates as highly active halogen-bonding-donor catalysts. *Chem. Commun.* **2018**, *54*, 10320–10323; b) Takeda, Y.; Hisakuni, D.; Lin, C.-H.; Minakata, S. 2-Halogenoimidazolium Salt Catalyzed Aza-Diels–Alder Reaction through Halogen-Bond Formation. *Org. Lett*. **2015**, *17*, 318–321; c) Jungbauer, S. H.; Walter, S. M.; Schindler, S.; Rout, L.; Kniep, F.; Huber, S. M. Activation of a carbonyl compound by halogen bonding. *Chem. Commun.* **2014**, *50*, 6281–6284.

[10] a) von der Heiden, D.; Detmar, E.; Kuchta, R.; Breugst, M. Activation of Michael Acceptors by Halogen-Bond Donors. *Synlett* **2018**, *29*, 1307–1313; b) Gliese, J.-P.; Jungbauer, S. H.; Huber, S. M. A halogen-bonding-catalyzed Michael addition reaction. *Chem. Commun.* **2017**, *53*, 12052–12055.

[11] a) Benz, S.; Poblador-Bahamonde, A. I.; Low-Ders, N.; Matile, S. Catalysis with Pnictogen, Chalcogen, and Halogen Bonds. *Angew. Chem. Int. Ed.* **2018**, *57*, 5408–5412; b) Dreger, A.; Engelage, E.; Mallick, B.; Beer, P. D.; Huber, S. M. The role of charge in 1,2,3-triazol(ium)-based halogen bonding activators. *Chem. Commun.* **2018**, *54*, 4013–4016; c) Jungbauer, S. H.; Huber, S. M. Cationic Multidentate Halogen-Bond Donors in Halide Abstraction Organocatalysis: Catalyst Optimization by Preorganization. *J. Am. Chem. Soc.* **2015**, *137*, 12110–12120; d) Kniep, F.; Walter, S. M.; Herdtweck, E.; Huber, S. M. 4,4′-Azobis(halopyridinium) Derivatives: Strong Multidentate Halogen-Bond Donors with a Redox-Active Core. *Chem. Eur. J.* **2012**, *18*, 1306–1310; e) Kniep, F.; Rout, L.; Walter, S. M.; Bensch, H. K. V.; Jungbauer, S. H.; Herdtweck, E.; Huber, S. M. 5-Iodo-1,2,3-triazolium-based multidentate halogen-bond donors as activating reagents. *Chem. Commun.* **2012**, *48*, 9299–9301; f) Walter, S. M.; Kniep, F.; Herdtweck, E.; Huber, S. M. Halogen-Bond-Induced Activation of a Carbon–Heteroatom Bond. *Angew. Chem. Int. Ed.* **2011**, *50*, 7187–7191.

[12] For reviews, see: a) Breugst, M.; von der Heiden, D. Mechanisms in Iodine Catalysis. *Chem. Eur. J.*, **2018**, *24*, 9187–9199; b) Bulfield, D.; Huber, S. M. Halogen Bonding in Organic Synthesis and Organocatalysis. *Chem. Eur. J.*, **2016**, *22*, 14434–14450; c) Schindler, S.; Huber, S. M. Halogen Bonds in Organic Synthesis and Organocatalysis. *Top. Curr. Chem.*, **2014**, *359*, 167–203.

[13] a) von der Heiden, D.; Bozkus, S.; Klussmann, M.; Breugst, M. Reaction Mechanism of Iodine-Catalyzed Michael Additions. *J. Org. Chem.* **2017**, *82*, 4037–4043; b) Kee, C. W.; Wong, M. W. In Silico Design of Halogen-Bonding-Based Organocatalyst for Diels–Alder Reaction, Claisen Rearrangement, and Cope-Type Hydroamination. *J. Org. Chem.* **2016**, *81*, 7459–7470; c) Nziko, V. de P. N.; Scheiner, S. Catalysis of the Aza-Diels–Alder Reaction by Hydrogen and Halogen Bonds. *J. Org. Chem.* **2016**, *81*, 2589–2597; d) Breugst, M.; Detmar, E.; von der Heiden, D. Origin of the Catalytic Effects of Molecular Iodine: A Computational Analysis. *ACS Catal.* **2016**, *6*, 3203 – 3212.

[14] a) Kuwano, S.; Suzuki, T.; Hosaka, Y.; Arai, T. A chiral organic base catalyst with halogen-bonding-donor functionality: asymmetric Mannich reactions of malononitrile with N-Boc aldimines and ketimines. *Chem. Commun.* **2018**, *54*, 3847–3850; b) Arai, T.; Suzuki, T.; Inoue, T.; Kuwano, S. Chiral Bis(imidazolidine)iodobenzene (I-Bidine) Organocatalyst for Thiochromane Synthesis Using an Asymmetric Michael/Henry Reaction. *Synlett* **2017,** *28*, 122–127; c) Lindsay, V. N. G.; Charette, A. B. Design and Synthesis of Chiral Heteroleptic Rhodium(II) Carboxylate Catalysts: Experimental Investigation of Halogen Bond Rigidification Effects in Asymmetric Cyclopropanation. *ACS Catal.* **2012**, *2*, 1221–1225.

[15] a) Robinson, S. W.; Beer, P. D. Halogen bonding rotaxanes for nitrate recognition in aqueous media. *Org. Biomol. Chem*., **2017**, *15*, 153–159; b) Lim, J. Y. C.; Marques, I.; Ferreira, L.; Félix, V.; Beer, P. D. Enhancing the enantioselective recognition and sensing of chiral anions by halogen bonding. *Chem. Commun.* **2016**, *52*, 5527–5530; c) Tepper, R.; Schulze, B.; Jäger, M.; Friebe, C.; Scharf, D. H.; Görls, H.; Schubert, U. S. Anion Receptors Based on Halogen Bonding with Halo-1,2,3-triazoliums. *J. Org. Chem.* **2015**, *80*, 3139–3150.

[16] For recent reviews, see: a)H. B. Jalani, A. C. Karagöz, S. B. Tsogoeva, *Synthesis* **2017**, *49*, 29-41; b) B. Schulze, U. S. Schubert, *Chem. Soc. Rev*. **2014**, *43*, 2522-2571.

[17] Nepal, B.; Scheiner, S. Competitive Halide Binding by Halogen Versus Hydrogen Bonding: Bis-triazole Pyridinium. *Chem. Eur. J.* **2015**, *21*, 13330–13335.

[18] Kaasik, M.; Kaabel, S.; Kriis, K.; Järving, I.; Aav, R.; Rissanen, K.; Kanger, T. Synthesis and Characterisation of Chiral Triazole-Based Halogen-Bond Donors: Halogen Bonds in the Solid State and in Solution. *Chem. Eur. J*. **2017**, *23*, 7337–7344.

[19] For reviews on asymmetric aza-Diels-Alder reactions, see: a) Eschenbrenner-Lux, V.; Kumar, K.; Waldmann, H. The Asymmetric Hetero-Diels–Alder Reaction in the Syntheses of Biologically Relevant Compounds. *Angew. Chem. Int. Ed.* **2014**, *53*, 11146–11157; b) Masson, G.; Lalli, C.; Benohouda, M.; Dagousset, G. Catalytic enantioselective [4 + 2]-cycloaddition: a strategy to access aza-hexacycles. *Chem. Soc. Rev*. **2013**, *42*, 902–923.

[20] Hein, J. E.; Tripp, J. C., Krasnova, L. B.; Sharpless, K. B.; Fokin, V. V. Copper(I)-Catalyzed Cycloaddition of Organic Azides and 1-Iodoalkynes. *Angew. Chem. Int. Ed.* **2009**, *48*, 8018-8021.

[21] Kuijpers, B. H. M.; Dijkmans, G. C. T.; Groothuys, S.; Quaedflieg, P. J. L. M.; Blaauw, R. H.; van Delft, F. L.; Rutjes, F. P. J. T. Copper(I)-Mediated Synthesis of Trisubstituted 1,2,3-Triazoles. *Synlett*. **2005**, 3059–3062.

[22] Worrell, B. T.; Hein, J. E.; Fokin, V. V. Halogen Exchange (Halex) Reaction of 5-Iodo-1,2,3-triazoles: Synthesis and Applications of 5-Fluorotriazoles. *Angew. Chem. Int. Ed*. **2012**, *51*, 11791–11794.

[23] Gaussian 09, Revision D.01, Frisch, M. J.; Trucks, G. W.; Schlegel, H. B.; Scuseria, G. E.; Robb, M. A.; Cheeseman, J. R.; Scalmani, G.; Barone, V.; Mennucci, B.; Petersson, G. A.; Nakatsuji, H.; Caricato, M.; Li, X.; Hratchian, H. P.; Izmaylov, A. F.; Bloino, J.; Zheng, G.; Sonnenberg, J. L.; Hada, M.; Ehara, M.; Toyota, K.; Fukuda, R.; Hasegawa, J.; Ishida, M.; Nakajima, T.; Honda, Y.; Kitao, O.; Nakai, H.; Vreven, T.; Montgomery, J. A., Jr.; Peralta, J. E.; Ogliaro, F.; Bearpark, M.; Heyd, J. J.; Brothers, E.; Kudin, K. N.; Staroverov, V. N.; Kobayashi, R.; Normand, J.; Raghavachari, K.; Rendell, A.; Burant, J. C.; Iyengar, S. S.; Tomasi, J.; Cossi, M.; Rega, N.; Millam, J. M.; Klene, M.; Knox, J. E.; Cross, J. B.; Bakken, V.; Adamo, C.; Jaramillo, J.; Gomperts, R.; Stratmann, R. E.; Yazyev, O.; Austin, A. J.; Cammi, R.; Pomelli, C.; Ochterski, J. W.; Martin, R. L.; Morokuma, K.; Zakrzewski, V. G.; Voth, G. A.; Salvador, P.; Dannenberg, J. J.; Dapprich, S.; Daniels, A. D.; Farkas, Ö.; Foresman, J. B.; Ortiz, J. V.; Cioslowski, J.; Fox, D. J. Gaussian, Inc., Wallingford CT, **2009**.
[24] Yanai, T.; Tew, D.; Handy, N. A new hybrid exchange–correlation functional using the Coulomb-attenuating method. *Chem. Phys. Lett.* **2004**, *393*, 51-57.
[25] Zhao, Y.; Truhlar, D. G. The M06 suite of density functionals for main group thermochemistry, thermochemical kinetics, noncovalent interactions, excited states, and transition elements: two new functionals and systematic testing of four M06-class functionals and 12 other functionals. *Theor. Chem. Acc.* **2008**, *120*, 215-241.
[26] Weigend, F.; Ahlrichs, R. Balanced basis sets of split valence, triple zeta valence and quadruple zeta valence quality for H to Rn: Design and assessment of accuracy. *Phys. Chem. Chem. Phys.* **2005**, *7*, 3297-3305.
[27] Lu, T.; Chen, F. Multiwfn: A multifunctional wavefunction analyzer. *J. Comput. Chem.* **2012**, *33*, 580-592.
[28] Varetto, U. Molekel 5.4.
[29] The **7a** + **TBACl** complex precipitates at 0.4 M concentration, if the reaction was run under ten times diluter conditions the complex was still in solution, however no reaction took place
[30] Surprisingly, Minakata *et al.* observed a reverse trend between halogen atom polarisability and catalytic activity in reference 9a.
[31] This was in addition to the 20 minute delay in adding the diene **2** after solubilising the catalyst present in the other reactions
[32] Zhang, X.; Hao, X.; Liu, L.; Pham, A.-T.; López-Andarias, J.; Frontera, A.; Sakai, N.; Matile, S. Primary Anion−π Catalysis and Autocatalysis. *J. Am. Chem. Soc.* **2018**, *140*, 17867-17871.
[33] Pilli; R. A.; Russowsky. D. Secondary Mannich bases *via* trimethylsilyl trifluoromethanesulphonate promoted addition of silyl enol ethers to Schiff bases. *Chem. Commun*., **1987**, 1053-1054.
[34] Kawęcki. R. Aza Diels–Alder reactions of sulfinimines with the Rawal diene. *Tetrahedron: Asymmetry* **2006**, *17*, 1420–1423.
[35] For reviews see: a) Krossing, I.; Raabe, I. Noncoordinating Anions—Fact or Fiction? A Survey of Likely Candidates, *Angew. Chem. Int. Ed.* **2004**, *43*, 2066–2090; b) Strauss, S. H. The Search for Larger and More Weakly Coordinating Anions. *Chem. Rev.* 1993, 93, 927-942.
[36] Saito, M.; Tsuji, N.; Kobayashi, Y.; Takemoto, Y. Direct Dehydroxylative Coupling Reaction of Alcohols with Organosilanes through Si–X Bond Activation by Halogen Bonding. *Org. Lett*. **2015**, *17*, 3000–3003;
[37] Surprisingly, in reference 9a tetrafluoroborate containing triazolium salts were used to catalyse aza-Diels-Alder reaction. The authors claim that steric bulk of the substituents on the triazolium ring influence significantly the catalytic activity of the salts. In the paper, the less sterically crowded catalysts (that are more comparable to our compounds **8**) gave lower yields than those that were more crowded.
[38]We were able to recover 80% of the catalyst after the reaction, see SI Figure S45B.
[39] Compounds with m/z ratios corresponding to intermediates **13**/**14**/**17** and **15**/**16** were detected by HRMS in the reaction mixture. By HMBC we infer that a methylene group is nearby to a carbonyl group in the intermediate, which cannot be possible in the case of intermediate **16**. We speculate that the TMS substituent is located on the nitrogen atom in **14** based on the observation that **14** is quite persistant in the reaction medium in the case of hydrogen containing triazole salt **12**. All attempts at isolating the intermediate were unsucsessful. For furter details see SI.
[40] Girling, P. R.; Kiyoi, T.; Whiting, A. Mannich–Michael *versus* formal aza-Diels–Alder approaches to piperidine derivatives. *Org. Biomol. Chem.* **2011**, *9*, 3105–3121.
[41] Freitas, L. B. de O.; Eisenberger, P.; Crudden, C. M. Mesoionic Carbene–Boranes. *Organometallics* **2013**, *32*, 6635–6638.

For Table of Contents Only